The m4 gene of murine gammaherpesvirus modulates productive and latent infection in vivo

JOURNAL OF VIROLOGY, Jan. 2004, p. 758–767 Vol. 78, No. 2
0022-538X/04/$08.00+0 DOI: 10.1128/JVI.78.2.758–767.2004

The M4 Gene of Murine Gammaherpesvirus Modulates Productive and Latent Infection In Vivo

A. C. Townsley, B. M. Dutia, and A. A. Nash*

Laboratory for Clinical and Molecular Virology, University of Edinburgh, Summerhall, Edinburgh EH9 1QH, United Kingdom

Received 28 July 2003/Accepted 30 August 2003

Murine gammaherpesvirus 68 (MHV-68) infection of mice represents a viable small-animal model for the study of gammaherpesvirus pathogenesis. MHV-76 is a deletion mutant of MHV-68, which lacks four MHV-68-specific genes (M1 to M4) and eight viral tRNA-like sequences at the 5′ end of the genome. These genes are implicated in latency and/or immune evasion. Consequently, MHV-76 is attenuated in the acute phase of in vivo infection with respect to MHV-68. Little is known about the role of M4 in viral infection, except that it is expressed as an immediate-early/early transcript during lytic replication of MHV-68 in vitro. To elucidate the contribution M4 makes to in vivo pathogenesis, we created a novel MHV-76 mutant (MHV-76inM4), in which the region of MHV-68 coding for M4 and accompanying putative promoter elements were inserted into the 5′ region of the MHV-76 genome. The growth of MHV-76inM4 in vitro was indistinguishable from that of MHV-76 and MHV-68. However, virus titers from MHV-76inM4-infected BALB/c mice were significantly increased with respect to MHV-76 at early times in the lung. In addition, at days 17 and 21 postinfection, there was a significant elevation in latent viral load in splenocytes of MHV-76inM4-infected mice compared to MHV-76. Like MHV-76-infected mice, MHV-76inM4-infected mice display no evidence of overt splenomegaly, a finding characteristic of MHV-68 infection. M4 expression in vivo was detectable during productive infection in the lung and during the establishment of latency in the spleen, but in general M4 was not detectable during long-term latency (day 100 postinfection).

Murine gammaherpesvirus 68 (MHV-68) is a well-established small-animal model for the study of gammaherpesvirus pathogenesis. MHV-68 infects inbred and outbred mice and, after intranasal administration, undergoes productive infection within lung epithelia, followed by lifelong latent infection. B lymphocytes within the spleen comprise the major reservoir of latent virus after intranasal infection (9, 27) although, like Kaposi's sarcoma-associated herpesvirus, latent virus is detectable within several other cell types, specifically dendritic cells, macrophages/monocytes, and lung epithelia (8, 21, 35). After the initial detection of latently infected cells, the splenic viral latent load continues to increase and then begins to decrease after it reaches a peak at approximately 14 days postinfection (p.i.). We refer to this stage of infection as acute-phase latency. During acute-phase latency, overt splenomegaly is evident, a process dependent on host ($CD4^+$ T cells) and viral factors (13, 25).

A related and previously characterized murid herpesvirus, MHV-76, replicates equivalently to MHV-68 in vitro. However, MHV-76 is phenotypically distinguishable from MHV-68 after infection of immunocompetent mice. Lytic replication in the lung differs significantly from MHV-68, since MHV-76 displays accelerated clearance and an increased inflammatory infiltrate. Acute-phase splenic latency is also affected, with peak latency reduced ~50-fold with respect to MHV-68. Significantly, splenomegaly is profoundly reduced in MHV-76-infected mice. Macrae et al. (13) have confirmed this altered phenotype of MHV-76 is the result of a 9,538-bp deletion at the left terminus of MHV-68. In MHV-68, this 9,538-bp encompasses four open reading frames (ORFs; M1 to M4) and eight viral tRNA-like sequences. This locus represents a cluster of MHV-68-specific genes (possibly with latency-associated or immunoregulatory functions), a genomic structure akin to other characterized gammaherpesviruses, where virus-specific genes are interspersed between gene blocks conserved among gammaherpesviruses (31). Aside from this deletion, the left termini of the MHV-76 and MHV-68 genomes are effectively identical, but for one amino acid substitution and a trivial discrepancy between terminal repeats. Reinsertion of the deleted 9,538 bp into MHV-76 restored the in vivo phenotype to that of MHV-68 (13). Furthermore, an independently isolated MHV-68 mutant, with a similar deletion to that of MHV-76, displays a similar defect in splenic latency (4), underscoring the contribution this locus at the left terminus of MHV-68 makes to in vivo pathogenesis.

Data concerning the involvement of these MHV-68-specific elements during in vivo infection remains limited. Thus far, only one gene remains functionally characterized: M3 encodes a broad-spectrum chemokine-binding protein that is expressed during lytic replication and persistence (16, 30). Recombinant MHV-68 mutants containing targeted loss-of-function mutations provide data on the contribution of virus-specific ORFs to in vivo pathogenesis. A deletion mutant lacking the M3 gene suggests an important role for M3 in the maintenance of a normal splenic latent load (2), although another deletion mutant did not reproduce this phenotype but did demonstrate a role for M3 in the modulation of the inflammatory response after intracranial infection (29). Similarly, M1 has been implicated in the control of reactivation (5), and a virus deficient in functional M2 protein shows a major defect in splenic latency (11).

* Corresponding author. Mailing address: Laboratory for Clinical and Molecular Virology, University of Edinburgh, Summerhall, Edinburgh EH9 1QH, United Kingdom. Phone: 44-131-650-6164. Fax: 44-131-650-6511. E-mail: aanash@staffmail.ed.ac.uk.

Little is known about the properties of the M4 gene except that it is expressed as an immediate-early transcript during lytic infection in vitro and that expression in vivo has been detected during lytic infection but not during long-term persistence (6, 32). Considering the genomic location of M4 and that it is dispensable for in vitro replication (13), it is likely that the M4 gene encodes a protein that is involved during latency or has some immunomodulatory role during infection in vivo. The current experiments used a novel approach to assess the contribution M4 makes to MHV-68 pathogenesis in vivo, utilizing a recombinant MHV-76 mutant expressing the M4 gene under the control of its native promoter. This recombinant virus demonstrates that M4 influences productive infection in the lung and acute-phase latency within the spleen. To our knowledge, this is the first report of a role for the M4 gene product in the pathogenesis of a MHV-68 infection.

MATERIALS AND METHODS

Virus stocks and mouse infections. Virus stocks of MHV-68 and MHV-76 were prepared by infection of BHK-21 cells with MHV-68 clone g2.4 (1, 7) or MHV-76 (1, 13) at a low multiplicity of infection (MOI; 0.001 PFU/cell) as previously described (23). Viral DNA used for electroporation, sequencing, and Southern analysis was extracted from intact purified virions as described previously (7). Female BALB/c mice were purchased from B&K Universal (Hull, United Kingdom) and were infected at 4 weeks of age. All mice were infected intranasally under halothane anesthesia by administration of 4×10^5 PFU of virus suspended in 40 μl of sterile phosphate-buffered saline. At specific times p.i., mice were euthanized by CO_2 asphyxiation, and organs were harvested. Lung tissue was frozen at −70°C until assays were performed.

Analysis of infected tissues. For determining levels of preformed infectious virus, the method described by Sunil-Chandra et al. (23) was used. Briefly, tissues were homogenized in Glasgow medium, supplemented with 10% newborn calf serum, 100 U of penicillin/ml, 100 U of streptomycin/ml, 2 mM L-glutamine, and subjected to one freeze-thaw cycle. Plaque assays to detect preformed virus were performed as previously described (23) on BHK-21 monolayers. An ex vivo reactivation assay was utilized to detect latent virus within splenocytes, as described previously (23). Briefly, splenocytes were counted, and specific dilutions incubated with a susceptible monolayer (BHK-21 cells). Reactivating virus was calculated from the total number of countable plaques minus the contribution from preformed infectious virus. Preformed infectious virus was determined by subjecting splenocytes to one freeze-thaw cycle prior to titration by plaque assay. No preformed infectious virus was detectable from any splenocyte sample after day 5 p.i.

Generation of recombinant viruses. MHV-76inM4 was generated by cotransfection of BHK-21 cells with MHV-76 DNA and digested plasmid DNA. The appropriate plasmid was generated by subcloning an MHV-68 terminal repeat fragment (22) into the *Pst*I site in the polylinker region of pUC18. A defined region of the MHV-68 genome encompassing the M4 ORF (nucleotides [nt] 7414 to 10914, accession no. U97553) was inserted downstream between the *Bam*HI and *Eco*RI sites. To facilitate directional subcloning of the M4 fragment into pUC18, restriction endonuclease sites were added to the M4 fragment of MHV-68 during PCR amplification. PCR was performed by using MHV-68 DNA as a template in the presence of 10 U of *Pfu* turbo polymerase (Stratagene), *Pfu* Turbo polymerase buffer (Stratagene), 100 μM deoxynucleoside triphosphate (dNTP), and 50 pmol of each of the following oligonucleotides: 5′-*GCGC*<u>*GGATCC*</u>CATGTGCTACCTCTGTGG-3′ (nt 7414 to 7432) and 5′-*GCGC*<u>*GAATTC*</u>GTACCGTCTGAGTGACTG-3′ (nt 10914 to 10897). The forward primer introduced a *Bam*HI site (underlined) within the PCR product, and the reverse primer introduced an *Eco*RI site (underlined). The italicized sequence represents sequence not found in the MHV-68 template DNA being amplified. Before electroporation, the plasmid was digested with *Hin*dIII and *Eco*RI (excising both the terminal repeat and M4 insert on the same fragment) and purified by phenol-chlorophorm extraction and ethanol precipitation. After electroporation of BHK-21 cells with MHV-76 DNA and digested plasmid DNA, the transfected BHK-21 cells were seeded into 96-well plates. Wells containing single plaques after 5 days of incubation were harvested, and half the volume of cell suspension was pelleted, resuspended in 100 μl of sterile phosphate-buffered saline, and subjected to overnight digestion with proteinase K at 56°C. Proteinase K was heat inactivated at 95°C for 10 min, and 10 μl of the sample was analyzed by PCR for the presence of M4 and ORF50. The M4 PCR utilized the primer pair M4AFor (5′-*GCGC*<u>*GGATCC*</u>GACACCTGGAGAAGATGATGATATTC-3′; nt 8616 to 8637) and M4ARev (5′-*CGC*<u>*GAATTC*</u>GGCAGTCGCATAACCATGTCCACG-3′; nt 9176 to 9155). The ORF50 PCR utilized the primer pair ORF50For (5′-ATGGCACATTTGCTGCAGAAC-3′; nt 68483 to 68503) and ORF50Rev (5′-ACGGCGCCTGTGTACTCAA-3′; nt 68838 to 68820). PCRs were setup by using 5 U of *Taq* DNA polymerase (Invitrogen) per reaction in the presence of 100 μM dNTP, 3 mM $MgCl_2$, 50 pmol of each primer, and *Taq* DNA polymerase buffer (Invitrogen). The cycling parameters were the same for both primer pairs: 94°C for 45 s, 56°C for 45 s, and 72°C for 60 s for 40 cycles, with a final extension at 72°C for 7 min. Single plaque isolates positive for M4 and ORF50 by PCR were diluted and reseeded onto BHK-21 monolayers within 96-well plates. After five rounds of single-plaque selection, isolates were screened for wild-type MHV-76 contamination by PCR. Genomic rearrangements were confirmed by sequencing of purified viral DNA, and Southern analysis was performed according to established procedures (19) with ^{32}P-labeled probes produced from a fragment of M4 (nt 8616 to 9176) and the *Hin*dIIIG fragment of MHV-68 (nt 11099 to 16237). Sequencing was carried out with IRD800-modified primers on a Li-Cor automated sequencer.

A revertant virus of MHV-76inM4 was produced by cotransfection of purified MHV-76inM4 DNA with the cosmid clone cM1, containing a fragment of the left end of MHV-76 (13). DNA was produced from single plaques as described above and was analyzed by using a multiplex PCR for M4 (primer pair M4AFor and M4ARev) and ORF50 (primer pair ORF50For and ORF50Rev). Reactions contained 50 pmol of each primer, and the cycling parameters were 94°C for 45 s, 56°C for 45 s, and 72°C for 60 s for 30 cycles, with a final extension at 72°C for 7 min. Genomic rearrangements were confirmed by Southern analysis, with the same probes as those used to analyze MHV-76inM4.

In vitro infections. Single-step and multistep growth in vitro was analyzed by infecting BHK-21 cells in suspension for 90 min at an MOI of 5 (single-step growth) or 0.05 (multistep growth). Cells were pelleted and resuspended in fresh complete Glasgow medium four times to remove unbound virus before they were seeded into 24-well plates. At specific times p.i., wells were harvested and infectious virus was determined by plaque assay, as described above. All infections were performed in duplicate, with each infection titrated in duplicate.

Northern analysis. RNA for Northern analysis was harvested from C127 cells infected in suspension in vitro with an MOI of 10. To inhibit early gene expression, C127 cells were treated with cycloheximide (CHX; 100 μg/ml) and to inhibit late gene expression, cells were treated with phosphonoacetic acid (PAA; 100 μg/ml). CHX- and PAA-treated samples were harvested 8 h p.i. Untreated samples were harvested 18 h p.i. RNA was extracted by using an RNeasy Minikit (Qiagen) according to the manufacturer's directions and then resuspended in RNase-free water. A total of 10 μg of total RNA was loaded in each lane and fractionated through 1.2% agarose gels containing 6.6% formaldehyde, 40 mM MOPS [3-(*N*-morpholino)propanesulfonic acid], 10 mM sodium acetate, and 1 mM EDTA. Blotting onto Hybond N^+ membranes was performed in the presence of 20× SSC (1× SSC is 0.15 M NaCl plus 0.015 M sodium citrate). ^{32}P-labeled double-stranded DNA probes specific for M4 (nt 8616 to 9176) and ORF50 (nt 68483 to 68838) were generated from purified PCR products. Hybridization was performed in Ultrahyb (Ambion) according to the manufacturer's directions.

RT-PCR. Tissues used for RNA extraction were snap-frozen in liquid nitrogen at the time of harvesting. RNA was extracted from tissues of infected BALB/c mice by using an RNeasy Minikit (Qiagen). Briefly, after RNA isolation, RNA was resuspended in RNase-free water and treated with 10 U of DNase I (DNA-free; Ambion) for 1 h at 37°C. Samples were repurified by using an RNeasy kit, and the resulting RNA was quantified by spectrophotometry (Cecil). RNA was analyzed by denaturing gel electrophoresis to determine RNA integrity. A total of 4 μg of the resulting RNA was subjected to a final incubation with 10 U of DNase I (DNA-free; Ambion) for 1 h at 37°C. A total of 2 μg of RNA was reverse transcribed with RNase H^- Superscript II (Invitrogen) in a final volume of 20 μl according to the manufacturer's instructions. A total of 2 μl of cDNA was used per PCR, with 5 U of *Taq* DNA polymerase (Invitrogen) per reaction in the presence of 100 μM dNTP, 3 mM $MgCl_2$, 50 pmol of each primer, and *Taq* polymerase buffer. PCR primers used were as described by Wakeling et al. (33), with the exception of the M4 primer pair, for which the M4AFor and M4ARev primers were used. The cycling parameters were the same for each primer pair set used: 94°C for 45 s, 57°C for 45 s, and 72°C for 40 s for 35 cycles, with a final extension at 72°C for 7 min. Reverse transcription-PCR (RT-PCR) products were separated by agarose gel electrophoresis and blotted onto Hybond N^+ membranes (Amersham) in the presence of 10× SSC prior to hybridization with

^{32}P-labeled DNA probes in Ultrahyb (Ambion) according to the manufacturer's directions.

Real-time PCR. Real-time PCR for the quantification of viral genome load was performed on a LightCycler (Roche), with the intercalating dye SYBR green to determine levels of double-stranded DNA product. A region of the ORF50 gene was amplified with specific primers (ORF50For and ORF50Rev), and all products from real-time PCR were analyzed by melting temperature to confirm specificity. DNA was extracted from splenocytes by using a Qiagen tissue kit, and 50 ng was used per PCR. Additional reactions were performed on a dilution series of a plasmid containing the entire ORF50 sequence, producing a standard curve to enable quantification of unknown samples. Standards were spiked with DNA isolated from the spleens of uninfected BALB/c mice, demonstrating that amplification efficiencies were comparable.

5′ and 3′ RACE. Rapid amplification of cDNA ends was performed as follows. Briefly, C127 cells were infected in vitro at an MOI of 10, and harvested 18 h p.i. RNA was extracted by using an RNeasy Minikit (Qiagen) as per manufacturers directions, and resuspended in RNase-free water. A total of 5 μg of the resulting RNA was treated with 10 U of DNase I (DNA-free; Ambion) for 1 h at 37°C. The resulting RNA was used directly in the First-Choice RLM-RACE (rapid amplification of cDNA ends) kit (Ambion). RACE PCR products were purified by using a Qiagen PCR purification kit and subcloned by using the TOPO-TA cloning kit (Invitrogen). Four reactions were sequenced for 5′ RACE, and three reactions sequenced for 3′ RACE. Identical sequencing data was obtained for all of the 5′-RACE products and for all of the 3′-RACE products. Sequencing was carried out with IRD800-modified primers on a Li-Cor automated sequencer.

Statistical analysis. Titer data and real-time PCR data were analyzed by using the nonparametric Mann-Whitney test.

RESULTS

Targeted insertion of the M4 gene. A fragment of MHV-68 spanning the predicted M4 ORF (MHV-68 sequence, nt 7414 to 10914) was selected for insertion into the left terminus of MHV-76, in the equivalent genomic location M4 occupies in MHV-68. This fragment contains an additional 995 bp upstream of the predicted M4 ORF (31), for inclusion of promoter elements to allow the M4 gene to be expressed under the control of its native promoter within MHV-76. The 3.5-kb insert has not been shown to encode any further transcripts in addition to M4 and does not include any sequence from the neighboring M3 ORF. The cloned M4 sequence was compared to the previously published sequence (31), and no base pair alterations were detected. To assess the involvement of the M4 gene in viral pathogenesis, a recombinant MHV-76 virus expressing M4 (MHV-76inM4) was generated as described in Materials and Methods. This resulted in a 2,125-bp insertion at the left end of MHV-76, containing the entire predicted M4 ORF and putative promoter elements. M4 was expressed under the control of its native promoter, since it was anticipated that by this approach M4 expression by MHV-76inM4 would reflect that of MHV-68. Furthermore, insertion of a foreign promoter (human cytomegalovirus major immediate-early promoter) has been suggested to cause inappropriate phenotypes. Thus, inclusion of the native promoter for M4 in MHV-76inM4 would allow for an accurate and uncomplicated analysis of the M4 gene product in vivo. After transfection and five rounds of single-plaque selection, the MHV-76inM4 stock was found by PCR to be homogeneous and negative for wild-type MHV-76 (data not shown). The genomic structure of MHV-76inM4 at the left terminus was determined by Southern analysis with purified viral DNA digested with *Bam*HI and a double digestion with *Not*I and *Bgl*II (Fig. 1). Hybridization with a ^{32}P-labeled M4 sequence-specific probe yielded the predicted 9.8-kb fragment after *Bam*HI digest. This fragment size matched that expected after an ~2-kb insertion in MHV-76.

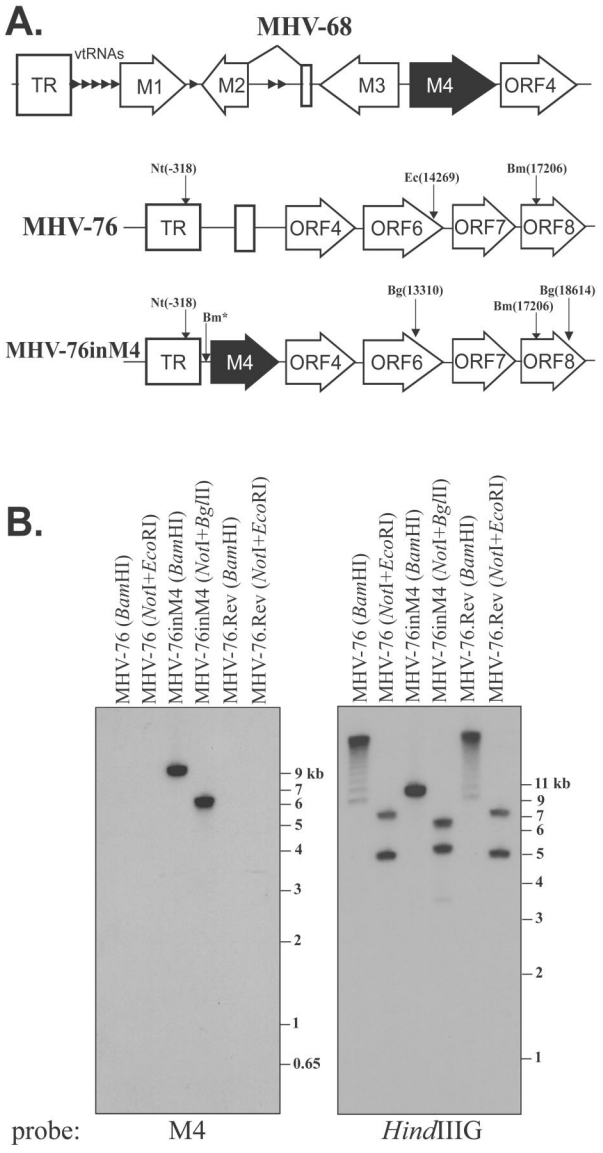

FIG. 1. Construction and verification of the genomic structures of MHV-76inM4 and MHV-76.Rev. (A) Structures of the left termini of the genomes of MHV-68, MHV-76inM4, and MHV-76. MHV-76inM4 were generated by the insertion of the MHV-68 sequence from nt 7414 to 10914 into the equivalent region in MHV-76. MHV-76.Rev was generated by restoring the MHV-76 sequence to MHV-76inM4, utilizing a cosmid clone containing a fragment of the left terminus of the MHV-76 genome. MHV-76 only contains the last 246 bp of the M4 ORF, whereas MHV-76inM4 contains the entire M4 ORF and putative promoter regions. The positions of restriction endonuclease sites (Bm, *Bam*HI; Nt, *Not*I; Ec, *Eco*RI; Bg, *Bgl*II) used to evaluate mutant virus DNA are shown. ✻, restriction site that derives from a small region of the polylinker site of pUC18 present within MHV-76inM4 (see Materials and Methods). (B) Southern analysis of the MHV-76, MHV-76inM4, and MHV-76.Rev genomes. Purified MHV-76 and MHV-76.Rev viral DNA was digested with either *Bam*HI or *Eco*RI+*Not*I, and MHV-76inM4 viral DNA was digested with either *Bam*HI or *Bgl*II+*Not*I. After electrophoresis and transfer, blots were hybridized with a ^{32}P-labeled probe spanning the M4 region (nt 8616 to 9176) and subsequently with a probe specific for a region conserved between each virus (nt 11099 to 16237). The results produced from Southern hybridization matched those predicted by sequence analysis (see Results).

Moreover, hybridization to one distinct fragment was consistent with an additional *Bam*HI site present in MHV-76inM4. This was as predicted, since a small region of the polylinker site of pUC18 (between the terminal repeat and M4 fragments) was expected to be present in MHV-76inM4. Furthermore, the M4 probe hybridized to the expected 6.2-kb fragment from the *Not*I-*Bgl*II digest. To conclusively determine the positioning of the M4 insertion and to assess whether any undesirable genomic rearrangements had occurred near the left terminus of MHV-76inM4 that may not have been detected with the M4 probe, a ^{32}P-labeled fragment of MHV-68 (*Hin*dIIIG fragment, bp 11099 to 16237, MHV-68 sequence) was used for probing. As expected, hybridization to fragments of predicted size followed *Hin*dIIIG probing. The *Hin*dIIIG probe hybridized to a 9.8-kb fragment from the *Bam*HI digest, matching the results seen with the M4 probe. Furthermore, hybridization to the predicted 5.3- and 6.2-kb fragments from the *Not*I-*Bgl*II digest confirmed the M4 fragment had recombined in the correct location. The results obtained from Southern blot analysis matched those predicted by sequence analysis exactly, verifying that the genomic structure at the left terminus of MHV-76inM4 was as anticipated. Finally, PCR and sequencing of purified MHV-76inM4 DNA further demonstrated that the insert had recombined in precisely the correct position, with no undesirable insertions or deletions detected. Overexposure of the blots did not indicate that any residual wild-type MHV-76 or genomically distinct subpopulation was present (data not shown).

To exclude the possibility that any phenotype of MHV-76inM4 was the result of a spurious mutation elsewhere in the genome and not a direct result of the insertion of M4, a revertant virus was generated (MHV-76.Rev). The genomic structure at the left end of MHV-76inM4 was restored to that of MHV-76 after cotransfection of purified MHV-76inM4 DNA with a cosmid fragment of MHV-76 (see Materials and Methods) and subsequent selection for single plaques negative for M4 by PCR. After transfection, a multiplex PCR-based screening method (M4 and ORF50) was used to select for MHV-76.Rev. Once single-plaque isolates were determined to be negative for M4 by PCR, they were subjected to a further three rounds of single-plaque selection to ensure homogeneity. The viral DNA was then subject to digestion with *Bam*HI and a double digestion with *Not*I and *Eco*RI prior to Southern blot analysis. Probing with a ^{32}P-labeled M4 sequence-specific probe yielded no detectable hybridization to either digested MHV-76 or MHV-76.Rev DNA, validating the multiplex PCR data. This confirmed that MHV-76.Rev contained no detectable M4 sequence and that the stock was free of contaminating MHV-76inM4. The *Hin*dIIIG probe hybridized to the predicted 8.9-kb fragment from the *Bam*HI digest, with terminal repeat laddering visible above this size (indicative of variable terminal repeat copy number). This banding pattern is consistent with the loss of the diagnostic *Bam*HI site in MHV-76inM4 and further establishes that MHV-76inM4 contains an ~2-kb insertion at the left end of the genome. Furthermore, the *Hin*dIIIG probe hybridized to the expected 5- and 7.5-kb fragments from the *Not*I-*Eco*RI digest (Fig. 1). Southern analysis of digested MHV-76 and MHV-76.Rev DNA gave indistinguishable results with both probes, indicating that MHV-76.Rev had reverted to the MHV-76 genotype.

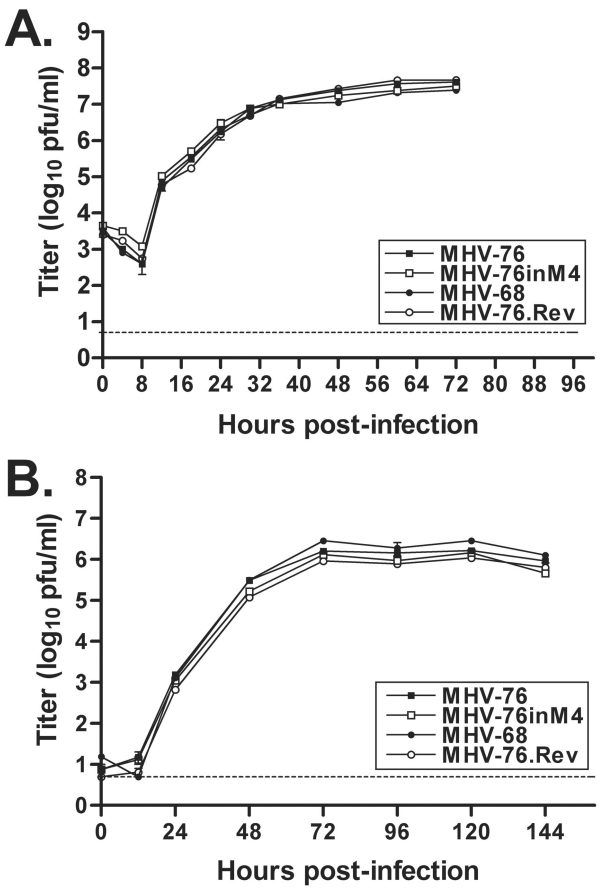

FIG. 2. MHV-76, MHV-68, MHV-76inM4, and MHV-76.Rev replicate equivalently in vitro. (A and B) Single-step growth curves (5 PFU/cell) (A) and multistep growth curves (0.05 PFU/cell) (B) were performed to determine any growth deficiencies or enhancements in vitro. Infected BHK-21 monolayers were harvested at specific times p.i. and freeze-thawed three times before titers were determined by plaque assay. The data represent the means ± the standard error of the mean (SEM), with the experiment performed in duplicate. The dashed line represents the limit of detection of the assay (5 PFU).

MHV-76inM4 and MHV-76.Rev replicate equivalently in vitro to MHV-76 and MHV-68. MHV-76 replicates indistinguishably from MHV-68 during single-step in vitro growth (13), indicating that the M1, M2, M3, and M4 genes and 8vtRNA-like sequences are dispensable for in vitro replication. As a result, it was predicted that the insertion of M4 into MHV-76 would not influence in vitro replication. Studies on a similar deletion mutant of MHV-68 have further established that M4 is not essential for in vitro growth (4). Nevertheless, to investigate whether MHV-76inM4 or MHV-76.Rev displayed any alterations in in vitro replication, we compared MHV-76inM4, MHV-76.Rev, MHV-76, and MHV-68 during a single round and during multiple rounds of replication in BHK-21 cells. In our study, analysis of single and multiple rounds of replication demonstrated that all viruses replicated equivalently (Fig. 2), confirming that M4 is dispensable for in vitro replication and does not influence cell-cell spread in vitro. Consequently, MHV-76inM4 and MHV-76.Rev have no de-

tectable differences in in vitro replication that could account for any change in phenotype in vivo.

Characterization of M4 transcription by MHV-68 and MHV-76inM4. The M4 ORF was originally assigned after analysis of the sequenced MHV-68 genome (31) and was predicted to span coordinates 8409 to 9785. However, the analysis predicted putative ORFs and no studies to date have defined whether the predicted M4 ORF corresponds to the actual M4 ORF. Of interest was the possibility of an alternative translational start site downstream of that previously predicted. By RACE analysis, we determined the M4 transcript to initiate at sequence 8526 and terminate at sequence 9866. Therefore, position 8538 most likely represents the true translational start site, since the predicted translational start site of 8409 is absent from the transcript. This alternative ATG-initiated ORF at position 8538 has a putative TATA box 27 bp upstream of the beginning of the M4 transcript (position 8526). Furthermore, this translational start site has a stricter Kozak sequence than the previously predicted translational start site of position 8409. The above results demonstrate that the true M4 ORF spans from positions 8538 to 9785, differing from that predicted by Virgin et al. (31).

Ebrahimi et al. (6) have previously characterized M4 as an immediate-early transcript, expressed abundantly during lytic replication in vitro. We sought to establish that MHV-76inM4 is capable of M4 expression and that the pattern of M4 expression from MHV-76inM4 after in vitro infection is comparable to MHV-68. The promoter regions for M4 remain uncharacterized, and our inclusion of 1112 bp upstream from the transcriptional start site cannot definitively ensure M4 expression equivalent to MHV-68. Furthermore, the influence of neighboring genes within MHV-68 (M1 to M3) on the regulation of M4 expression is unknown. To exclude the possibility that the kinetic class or level of M4 transcription differed significantly between MHV-76inM4 and MHV-68, Northern analysis was performed on RNA extracted from C127 cells infected in vitro (MOI = 10) (Fig. 3). CHX- and PAA-treated samples were included to determine the kinetic class of the M4 transcripts expressed from MHV-76inM4 and MHV-68. Hybridization with a ^{32}P-labeled M4 sequence-specific probe detected a dominant ~1.4-kb transcript from MHV-68 and MHV-76inM4 samples, but not from the MHV-76-, MHV-76.Rev-, and mock-infected samples. M4 transcription from the CHX-treated MHV-68 and MHV-76inM4 samples is approaching the limit of detection of Northern analysis, since only weak signals were detectable from these lanes after hybridization with the M4 probe. Nevertheless, the presence of M4 expression in these samples is in agreement with previous observations that M4 can be transcribed in the absence of protein synthesis (6). However, the distinct ~1.4-kb transcript is more abundant in the PAA-treated samples than in the CHX-treated samples. Thus, despite limited transcription in the absence of protein synthesis, the majority of M4 transcription requires de novo protein synthesis; we therefore propose that M4 be classified as an immediate-early/early transcript. A ^{32}P-labeled ORF50 sequence-specific probe detected a distinct ~2-kb band of equivalent intensity in all samples, with the exception of the mock. This result is consistent with previous observations of ORF50 transcription in vitro (12). Ethidium bromide staining of the gel prior to blotting indicated that all lanes contained equivalent amounts of rRNA (data not shown). Probes specific for housekeeping genes (GAPDH [glyceraldehyde-3-phosphate dehydrogenase] and β-actin) gave inconsistent results for RNA extracted from cells infected with virus overnight. This is likely due to virus-induced shutoff of host transcription as previously observed (6). Therefore, ORF50 was used as a control for RNA loading when MHV-68 is compared with MHV-76 and mutant virus RNA. Hence, Northern analysis shows that M4 is expressed abundantly in vitro and that no significant differences are detectable in the expression of M4 in vitro by MHV-68 and MHV-76inM4 with respect to kinetic class and level of transcription.

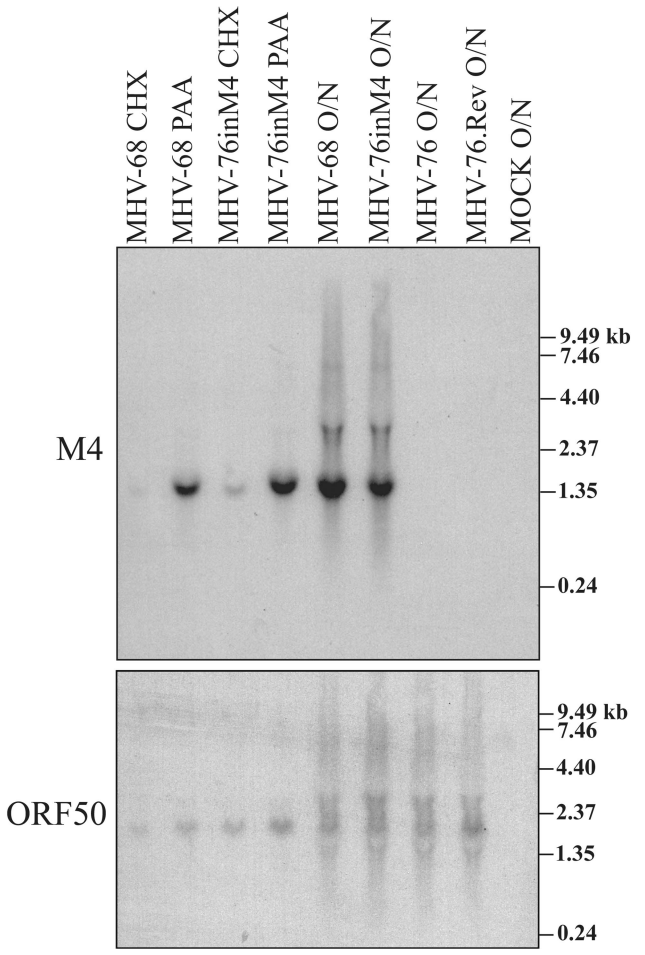

FIG. 3. Northern analysis of M4 transcription demonstrates that M4 encodes an immediate-early mRNA. C127 cells were infected in suspension at an MOI of 10 for 1 h (with or without inhibitors) before incubation at 37°C for 8 h (treated samples) or 18 h (untreated samples) prior to RNA extraction. Infected cells were either left untreated, treated with CHX (100 μg/ml) to inhibit protein synthesis, or treated with PAA (100 μg/ml) to inhibit DNA synthesis. Total RNA was harvested at the desired time p.i. and analyzed by Northern analysis. The blot was hybridized with a ^{32}P-labeled probe spanning the M4 region (nt 8616 to 9176), and with a ^{32}P-labeled probe spanning the ORF50 region (nt 68483 to 68838) to assess RNA loading and integrity (see Results).

MHV-76inM4 has increased lung titers at early times after intranasal infection. After intranasal infection of immunocompetent mice, MHV-76 is cleared more rapidly from the lung

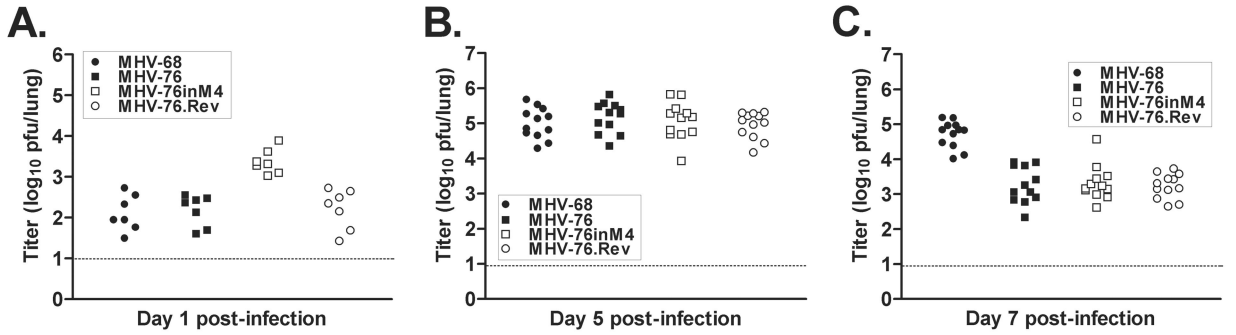

FIG. 4. MHV-76inM4 has a distinct phenotype during productive infection of the lung. BALB/c mice were infected intranasally with 4×10^5 PFU of virus, and lungs were harvested at day 1 (A), day 5 (B), and day 7 (C) p.i. The data shown are compiled from two (day 1) or three (days 5 and 7) independent experiments with three to four mice each. Virus titers were determined by plaque assay on BHK-21 monolayers. The data represent the viral titers from individual mice. The dashed line represents the limit of detection of the assay (10 PFU).

than MHV-68, suggesting that at least one element at the left terminus of MHV-68 contributes to delaying viral clearance. To assess any role for the M4 gene product during acute infection, BALB/c mice were infected intranasally with 4×10^5 PFU of virus, and viral titers were quantified by plaque assay from lungs harvested at specific times p.i. (days 1, 5, and 7). Figure 4 demonstrates that MHV-76inM4 was cleared from the lungs of infected mice with kinetics similar to those of MHV-76, as evidenced by reduced lung titers at day 7 p.i. in comparison to MHV-68. Thus, M4 does not appear to be involved in delaying viral clearance during productive infection of the lung. Lung titers at day 5 p.i. were equivalent for all viruses, establishing that MHV-76inM4 and MHV-76.Rev were capable of producing viral titers comparable to MHV-76 and MHV-68 during the peak of productive infection (Fig. 4). In contrast, at day 1 p.i., lung titers from MHV-76inM4-infected mice were significantly elevated with respect to MHV-76 ($P = 0.0006$), MHV-76.Rev ($P = 0.0006$), and MHV-68 ($P = 0.0006$). These findings imply that M4 is important during the initial stages of productive infection with MHV-68. Lung titers were analyzed between days 14 and 31 to exclude the possibility of viral recrudescence. This was not observed since viral titers from all mice from these time points were below the limit of detection.

MHV-76inM4 exhibits a prolonged peak of infective centers during acute-phase splenic latency. To assess any role for M4 during latency in vivo, we infected BALB/c mice intranasally with 4×10^5 PFU of virus, and the levels of latent virus were determined at specific times p.i. by using an ex vivo reactivation assay. MHV-76 has a profound deficit in acute-phase splenic latency, with M4 (absent from MHV-76) therefore a candidate gene for contributing to viral pathogenesis during this phase of infection. The ex vivo reactivation assay results are shown in Fig. 5. MHV-68 infective centers were detectable from day 5 p.i. onward, with peak latency observed at day 14 p.i. In contrast, MHV-76 infective centers peaked at day 10 p.i., with peak latency markedly reduced with respect to MHV-68. MHV-76inM4 infective centers peaked at day 14 p.i., although the subsequent decline in infective centers observed with MHV-76 infection was not evident with MHV-76inM4; the peak level of MHV-76inM4 infective centers was maintained throughout days 14 to 21. However, by day 100 p.i., infective

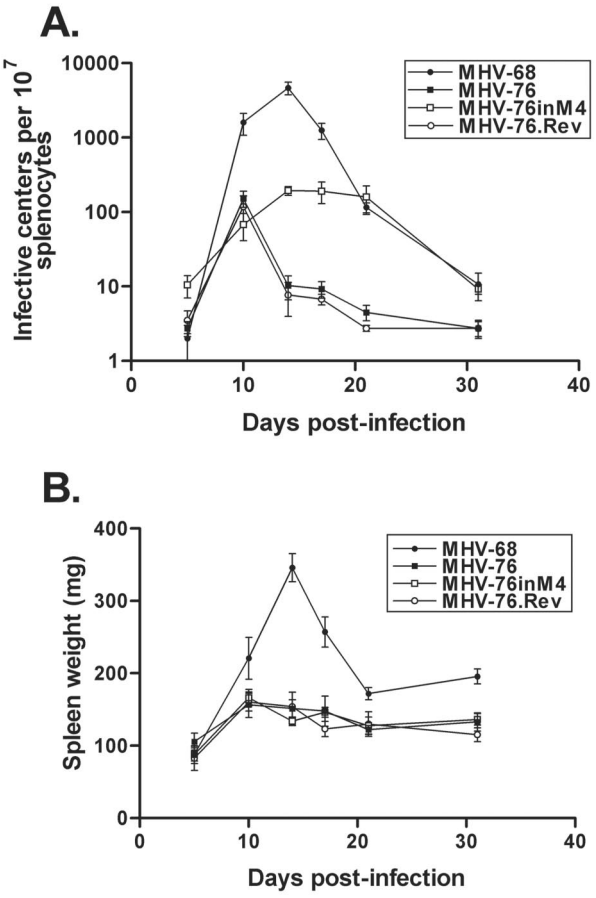

FIG. 5. M4 regulates acute-phase latency in vivo. BALB/c mice were infected intranasally with 4×10^5 PFU of virus, and latent virus was determined at specific times p.i. (A) The data shown represent latent virus (as measured by infective center assay) minus the infectious virus titer. The mean number of infective centers per 10^7 splenocytes (± the SEM) for four mice per group is shown at each time point. (B) The mean spleen weight (± the SEM) for four mice per group is shown for each time point. The data for both panels are from one of two independent experiments, with similar results obtained from both experiments.

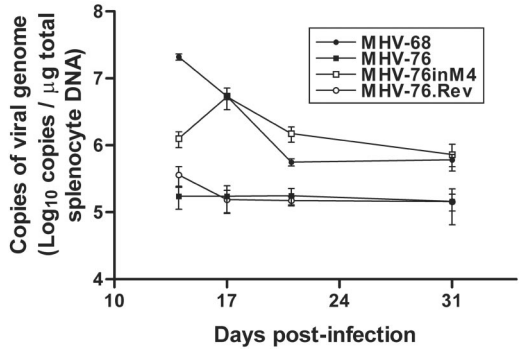

FIG. 6. MHV-76inM4 has an increased latent viral DNA load in the spleen in comparison to MHV-76. BALB/c mice were infected intranasally with 4×10^5 PFU of virus, and total DNA was extracted from splenocytes harvested at specific times p.i. Quantification of viral genomes was performed by real-time PCR analysis by using a LightCycler (Roche), with primers specific for the MHV-68 ORF50 gene. The mean copy number of viral genomes (± the SEM) for four mice per group is shown for each time point.

center data was equivalent for all viruses, suggesting that long-term latency was established at similar levels (data not shown). Overt splenomegaly during acute-phase latency is a well-documented phenotype accompanying MHV-68 infection (3, 8, 23), and this process has been demonstrated to increase the peak level of infective centres following MHV-68 infection (25). Splenomegaly is significantly reduced with MHV-76 infection in comparison to MHV-68 infection. Despite obvious differences in the patterns of acute-phase latency associated with MHV-76 and MHV-76inM4 infection, no evidence of significant splenomegaly was detectable with either virus, predicting little or no role for M4 in enhancing splenomegaly (Fig. 4).

MHV-76inM4 has an increased latent viral DNA load in the spleen. To confirm that the phenotype of MHV-76inM4 during acute-phase latency (as observed by reactivation assay) was the result of a difference in the level of latent virus and not solely due to an alteration in reactivation efficiency, real-time PCR was performed to quantify the viral genome load in splenocytes at days 14, 17, 21, and 31 p.i. The same splenocyte samples were used for both the reactivation assay and real-time PCR to allow a meaningful analysis. A portion of ORF50 was selected for amplification since it occupied a region distal to that affected by mutagenesis. The results are shown in Fig. 6. Melting analysis showed a specific melting peak for each sample at ~86°C, which corresponded to a distinct product of expected size after agarose gel electrophoresis (data not shown). At all time points analyzed, the spleens of MHV-76inM4-infected mice contained greater levels of latent viral DNA than MHV-76 or MHV-76.Rev. Specifically, at days 17 and 21 p.i., the difference in MHV-76inM4 viral genome load is statistically significant with respect to MHV-76 and MHV-76.Rev (day 17, $P < 0.029$; day 21, $P < 0.029$). Thus, a positive correlation between viral DNA copy number and reactivation assay data was observed at days 14 to 21 p.i. However, it is interesting that at day 17 p.i. MHV-68 and MHV-76inM4 differ considerably by reactivation assay and yet have equivalent viral genome copy numbers as determined by real-time PCR analysis.

M4 expression in vivo is detectable during lytic infection but not during persistence. To establish the pattern of M4 expression in vivo and whether such expression is compatible with the in vivo phenotype of MHV-76inM4, RT-PCR was performed on lung and spleen tissues from MHV-68-, MHV-76inM4-, and MHV-76.Rev-infected mice (Fig. 7). Expression in the lung was investigated at days 2, 4, and 14 p.i., encompassing both the acute-phase and resolution of productive infection. M4 expression in the spleen was analyzed at days 14, 21, and 100 p.i., covering both acute-phase latency and long-term persistence. Primers specific for the genes M4, ORF50, M11, and murine β-actin were used for analysis. ORF50 is only tran-

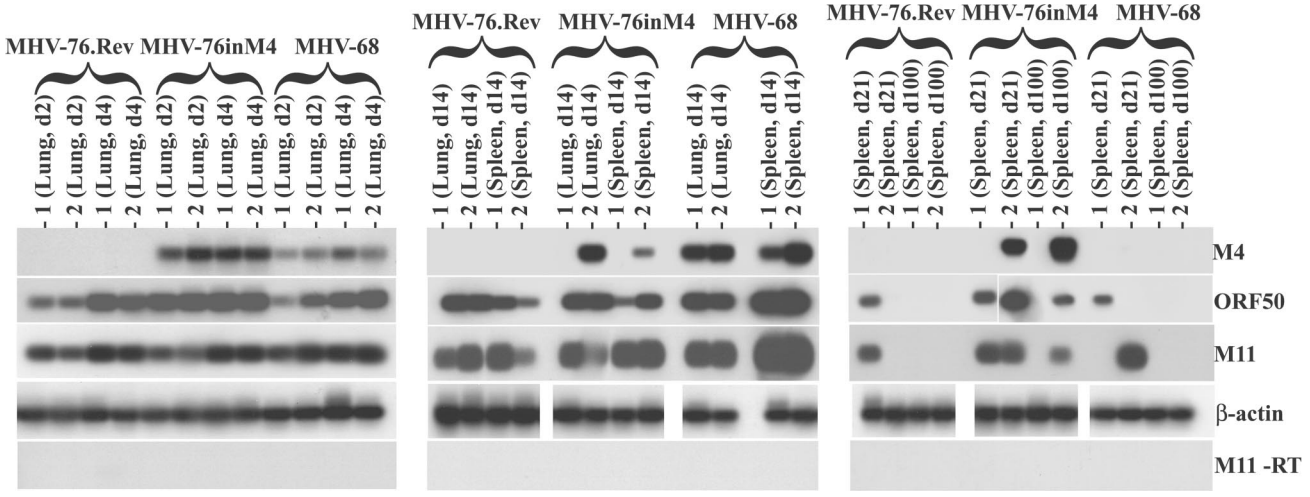

FIG. 7. In vivo transcription of M4. RNA was extracted from the lungs and spleens of BALB/c mice (two mice per virus per time point) at specific times p.i. RT-PCR was performed with primer sets specific for viral genes (M4, ORF50, and M11), in addition to murine β-actin. To confirm specificity, RT-PCR products were electrophoresed and subject to Southern blot analysis with ^{32}P-labeled gene-specific probes. For each RNA sample, reverse transcriptase was omitted in one case to control for the carryover of DNA (M11, no RT) prior to PCR and Southern blot analysis.

scribed during lytic infection, whereas M11 transcription has been detected during lytic infection and persistence (18, 33). β-Actin expression was abundant in all tissue samples, and control reactions performed without RT were uniformly negative. The sensitivity was determined by limiting dilution of PCR products generated with external primers and was determined to be between 1 and 10 copies in all cases. ORF50 expression by MHV-76inM4 at day 2 p.i. appeared more abundant in comparison to MHV-68 and MHV-76.Rev. This finding is consistent with plaque assay results establishing that MHV-76inM4-infected mice have elevated viral titers at this stage of infection. M4 was consistently detected during lytic infection in the lung from all MHV-76inM4 and MHV-68-infected mice but, within the spleen, M4 expression was less consistent; M4 expression was detectable in only one of two MHV-76inM4-infected mice at days 14 and 21 and in two of two MHV-68-infected mice at day 14. However, no M4 expression was detectable within the spleen at day 21 in MHV-68-infected mice. Importantly, M4 expression was always accompanied with ORF50 expression, which is in agreement with previous data demonstrating that M4 is not a latency-associated transcript (32). The presence of M4 transcription at day 100 p.i. in one MHV-76inM4-infected mouse is presumably the result of spontaneous reactivation or persistent low-level replication since ORF50 expression is evident. Thus, M4 expression by MHV-76inM4 and MHV-68 is consistently expressed during productive infection of the lung but is not consistently detectable during acute-phase splenic latency.

DISCUSSION

We have assessed here the role for the M4 gene product in vivo via a novel approach to MHV-68 mutagenesis. Insertion of the M4 gene into a deletion mutant of MHV-68 (MHV-76) produced a recombinant gammaherpesvirus (MHV-76inM4) expressing M4 similarly to MHV-68 in vitro, with a distinct phenotype during both productive infection in the lung, and during acute-phase latency in the spleen after intranasal infection of BALB/c mice. MHV-76inM4 exhibits elevated viral titers during productive infection in the lungs at 24 h p.i. and displays an increased latent load in the spleen during acute-phase latency compared to MHV-76. In addition, we have characterized the M4 transcript, characterizing both the initiation and termination sites of M4 transcription, and the temporal expression pattern in vitro.

Phenotype of MHV-76inM4 during productive infection in vivo. Preliminary sequence analysis of the MHV-68 genome led to the assignment of the putative M4 ORF. The genomic location of M4 and the absence of any obvious homolog led to the prediction that M4 may be important during infection in vivo (31). Two deletion mutants of MHV-68 lacking various elements, including the M4 ORF, replicate identically to MHV-68 in vitro, a finding consistent with the hypothesis that M4 is involved in pathogenesis in vivo (4, 13). Previous studies have detected M4 transcription during lytic infection in vivo but not during latent infection (20, 32). Our study is in agreement with such findings, since we were only able to detect M4 coexpressed with ORF50, a marker of lytic replication. However, we cannot exclude the possibility that M4 is expressed as a latent transcript by specific cell populations during acute-phase latency, whereas lytic replication is ongoing in different cell types. This is a possible scenario, since recent data demonstrate that M4 is expressed by several B-cell populations during acute-phase latency in the absence of ORF50 expression; in contrast, M4 expression by dendritic cells and macrophages was accompanied by ORF50 expression (14). Nevertheless, our data predict that M4 is not involved in the maintenance of long-term latent infection. It is not surprising that MHV-76inM4 exhibits a phenotype during productive infection of the lung, since M4 expression is readily detectable at this site during this phase of infection. MHV-76inM4 exhibits ~10-fold-higher lung titers at day 1 p.i. compared to MHV-76. This demonstrates that M4 plays an important role shortly after intranasal infection, possibly targeting an innate immune mechanism, such as alpha/beta interferons, macrophages/monocytes, natural killer cells or γδ T cells; the expression of M4 as an immediate-early transcript may be important for this early activity. It is interesting that MHV-68 does not exhibit an increase in viral titers 24 h p.i. compared to MHV-76, given that MHV-68 expresses M4 in a similar fashion to MHV-76inM4 at this time. However, since M1, M2, and M4 and the 8vtRNA-like sequences have not yet been functionally characterized, their influence on viral pathogenesis is unknown, particularly if expressed independently of one other. Thus, the combined effects of several gene products during the early phases of infection may explain the phenotypic differences between MHV-68 and MHV-76inM4 at 24 h p.i., since MHV-76inM4 lacks several elements present in MHV-68. Considering the intimate herpesvirus-host relationship, a more vigorous productive infection may not be advantageous, in evolutionary terms, to MHV-68; it may be detrimental to the host, jeopardizing the long-term carriage of the virus. M3, a soluble chemokine-binding protein encoded by MHV-68 but not MHV-76inM4, is expressed abundantly during productive infection and thus may have a role in influencing the early stages of productive infection. A recombinant vaccinia virus with a nonfunctional chemokine-binding protein exhibited significantly increased viral titers in vivo compared to the wild-type strain, demonstrating that specific viral immunoregulatory elements suppress maximal viral replication and virulence (17). Despite a possible elevation in ORF50 expression in MHV-76inM4-infected mice at day 2 p.i., it seems unlikely that an increase in ORF50 expression (which could enhance lytic replication) is responsible for the observed elevation in lung titers, since an accompanying elevation in M4 expression was also detectable, especially after gel electrophoresis of the PCR products prior to blotting (data not shown). Importantly, in vitro replication was equivalent for all viruses, with no detectable enhancement of MHV-76inM4 replication. A simpler explanation is that the increased viral titers and increased ORF50 expression are both markers of an enhanced productive infection.

Phenotype of MHV-76inM4 during acute-phase latency in the spleen. Since M4 was not readily detectable as a latency-associated transcript, it is interesting that MHV-76inM4 demonstrated a phenotype during acute-phase latency. The increase in infective centers from MHV-76inM4-infected mice at days 14 to 21 p.i., with respect to MHV-76, was in good agreement with the levels of latent viral genome copy number in the splenocyte population. Thus, MHV-76inM4 exhibits an elevated latent viral load in the spleen. In view of the reactivation

assay data, MHV-76inM4-infected mice most likely have an increased frequency of virus genome-positive cells in the spleen compared to MHV-76. However, one limitation of the real-time PCR analysis is that it was unable to determine the frequency of genome-positive splenocytes to unequivocally confirm this. Thus, the data suggest that M4 may be necessary for a maximal peak latent load during MHV-68 infection. One explanation for this phenotype is that a specific immune mechanism is responsible for the observed decline in infective centers with MHV-76 between days 10 and 14 p.i. If the M4 gene product inhibits the action of this immune mechanism, MHV-76inM4 would exhibit delayed clearance from the spleen. An alternative explanation, although one that we consider less likely given the phenotype in the lung, is that the phenotype in the spleen is the result of M4 actively contributing to the proliferation of latently infected cells, resulting in an increased latent load in spite of ongoing immune clearance. The stage of infection that the M4 gene product mediates its effect is unknown. The first possibility is that the M4 protein is having an effect at the times the phenotype is evident; however, M4 expression was variable between mice at the times the phenotype was observed. Therefore, M4 may only be produced in small amounts during acute-phase latency, suggesting that the M4 protein would have to be active in small quantities. A second explanation is that M4 may be an inherently stable protein able to persist in the splenic environment, having been produced principally during the establishment of splenic latency when lytic replication is more prevalent. If M4 does have immunomodulatory properties, this hypothesis suggests that the control of both productive and latent infection share a common immune mediator. Finally, it is conceivable that the phenotype observed in the spleen is the result of M4 expression during productive infection from a distal site other than the spleen. Expression of M4 within the lung or in the mediastinal lymph nodes draining the lung could result in an increased number of latently infected cells that may subsequently traffic to the spleen and give rise to an increased latent load.

Control of reactivation during acute-phase latency. It is clear that multiple factors influence the reactivation efficiency ex vivo. Previous studies have implicated virus-specific elements in the control of reactivation ex vivo; deletion mutants of MHV-68 frequently exhibit altered reactivation efficiencies ex vivo in comparison to wild-type MHV-68 (4, 5, 15). Furthermore, the observation that certain immune mechanisms appear to influence ex vivo reactivation implies host factors play a role in determining reactivation phenotype (24). In the present study, we observed differences in reactivation efficiency between MHV-68 and MHV-76inM4. Specifically, at day 17 p.i., the splenic viral latent loads of the two viruses are equivalent, whereas the reactivation efficiencies differed by ~7-fold. Given the close correlation between the reactivation assay and real-time PCR data, it seems likely that the difference in reactivation efficiency between MHV-68 and MHV-76inM4 observed at this time reflects an inherent ability of MHV-68 to reactivate better than MHV-76inM4 during acute-phase latency. Considering the different genomic structures of MHV-68 and MHV-76inM4, some element at the left terminus of MHV-68, other than M4, may augment reactivation efficiency during acute-phase latency. An MHV-68 mutant with a large deletion at the left terminus reactivates less efficiently from splenocytes during acute-phase latency than does MHV-68 (4). This finding is consistent with an element at the left end of MHV-68 having a role in altering reactivation efficiency.

MHV-68, between days 14 to 21 p.i., exhibits a decrease in viral latent load that mirrors the ex vivo reactivation data. This reduction in viral latent load (and reactivation) likely represents immune clearance of latent MHV-68. Conversely, MHV-76inM4 exhibits an increase in viral latent load between days 14 and 17 p.i. Since MHV-76 does not exhibit a significant decline in latent load akin to MHV-68, this rapid decline in viral latent load appears to be a feature of MHV-68 infection. It is possible that the higher latent load in splenocytes from MHV-68-infected mice elicits a greater immune response than MHV-76inM4, resulting in a more rapid eradication of latently infected splenocytes. Furthermore, only MHV-68 displays significant splenomegaly, and it is not known whether this amplification of lymphocytes influences the immune response to MHV-68. The M2 gene of MHV-68 is latency associated, is expressed predominantly by B lymphocytes during splenomegaly, and is a target for $CD8^+$ T cells (10). This could explain why MHV-76inM4 does not display a reduction in viral load between days 14 to 17, particularly if M2-specific $CD8^+$ T cells are found to be important for controlling MHV-68 during acute-phase latency. Alternatively, the differences between MHV-76inM4 and MHV-68 may reflect different states of latency. We consider it unlikely that the splenic phenotype associated with MHV-76inM4 is predominantly due to the establishment of latency in a different cell population from MHV-76, since it has been demonstrated that the vast majority of both latent MHV-76 and MHV-68 is present within the $CD19^+$-B-lymphocyte population (13). This indicates that the elements at the left end of MHV-68, absent in MHV-76, do not play a significant role in determining cellular tropism in the spleen.

At days 21 to 31 p.i., there is a significant decrease in reactivation observed with both MHV-68 and MHV-76inM4 without an equivalent decrease in viral latent load. We had originally predicted this decrease in reactivation to be the result of immune-mediated clearance of latently infected cells; however, real-time PCR data suggest otherwise. It has been proposed that specific immune mechanisms (gamma interferon in particular) are capable of influencing ex vivo reactivation efficiency (24), and this is one possibility that may explain the observed phenotype. Alternatively, the decrease in reactivation efficiency may simply reflect a transition to a more stable form of latency. It is noteworthy that latent virus recovered during acute-phase latency reactivates more efficiently than latent virus from mice in which long-term latency is established (34). One possibility is the existence of multiple latency programs, akin to Epstein-Barr virus, in which distinct patterns of gene expression can be identified during latency. Although no latency programs have been characterized for MHV-68, it does appear that several forms of latency exist in vivo (26, 28).

In conclusion, the data show that M4 is expressed as an immediate-early/early transcript and is expressed predominantly during productive infection in vivo. M4 modulates both productive infection in the lung at early times p.i. and levels of latent virus during acute-phase latency. This finding supports a possible role for M4 in immunoregulation, with the available

data suggesting that M4 may interfere with an innate immune mechanism. The functional characterization of M4 is currently under way in our laboratory.

ACKNOWLEDGMENTS

We thank Deborah Allen and Yvonne Ligertwood for technical assistance and Ian Bennet for sequencing.

A.C. Townsley is the holder of a Biotechnology and Biological Sciences Research Council studentship.

REFERENCES

1. **Blaskovic, D., M. Stancekova, J. Svobodova, and J. Mistrikova.** 1980. Isolation of five strains of herpesviruses from two species of free living small rodents. Acta Virol. **24:**468.
2. **Bridgeman, A., P. G. Stevenson, J. P. Simas, and S. Efstathiou.** 2001. A secreted chemokine binding protein encoded by murine gammaherpesvirus-68 is necessary for the establishment of a normal latent load. J. Exp. Med. **194:**301–312.
3. **Brooks, J. W., A. M. Hamilton-Easton, J. P. Christensen, R. D. Cardin, C. L. Hardy, and P. C. Doherty.** 1999. Requirement for CD40 ligand, $CD4^+$ T cells, and B cells in an infectious mononucleosis-like syndrome. J. Virol. **73:**9650–9654.
4. **Clambey, E. T., H. W. Virgin, and S. H. Speck.** 2002. Characterization of a spontaneous 9.5-kilobase-deletion mutant of murine gammaherpesvirus 68 reveals tissue-specific genetic requirements for latency. J. Virol. **76:**6532–6544.
5. **Clambey, E. T., H. W. Virgin, and S. H. Speck.** 2000. Disruption of the murine gammaherpesvirus 68 M1 open reading frame leads to enhanced reactivation from latency. J. Virol. **74:**1973–1984.
6. **Ebrahimi, B., B. M. Dutia, K. L. Roberts, J. J. Garcia-Ramirez, P. Dickinson, J. P. Stewart, P. Ghazal, D. J. Roy, and A. A. Nash.** 2003. Transcriptome profile of murine gammaherpesvirus-68 lytic infection. J. Gen. Virol. **84:**99–109.
7. **Efstathiou, S., Y. M. Ho, and A. C. Minson.** 1990. Cloning and molecular characterization of the murine herpesvirus 68 genome. J. Gen. Virol. **71**(Pt. 6)**:**1355–1364.
8. **Flano, E., S. M. Husain, J. T. Sample, D. L. Woodland, and M. A. Blackman.** 2000. Latent murine gamma-herpesvirus infection is established in activated B cells, dendritic cells, and macrophages. J. Immunol. **165:**1074–1081.
9. **Flano, E., I. J. Kim, J. Moore, D. L. Woodland, and M. A. Blackman.** 2003. Differential gamma-herpesvirus distribution in distinct anatomical locations and cell subsets during persistent infection in mice. J. Immunol. **170:**3828–3834.
10. **Husain, S. M., E. J. Usherwood, H. Dyson, C. Coleclough, M. A. Coppola, D. L. Woodland, M. A. Blackman, J. P. Stewart, and J. T. Sample.** 1999. Murine gammaherpesvirus M2 gene is latency-associated and its protein a target for $CD8^+$ T lymphocytes. Proc. Natl. Acad. Sci. USA **96:**7508–7513.
11. **Jacoby, M. A., H. W. Virgin, and S. H. Speck.** 2002. Disruption of the M2 gene of murine gammaherpesvirus 68 alters splenic latency following intranasal, but not intraperitoneal, inoculation. J. Virol. **76:**1790–1801.
12. **Liu, S., I. V. Pavlova, H. W. Virgin, and S. H. Speck.** 2000. Characterization of gammaherpesvirus 68 gene 50 transcription. J. Virol. **74:**2029–2037.
13. **Macrae, A. I., B. M. Dutia, S. Milligan, D. G. Brownstein, D. J. Allen, J. Mistrikova, A. J. Davison, A. A. Nash, and J. P. Stewart.** 2001. Analysis of a novel strain of murine gammaherpesvirus reveals a genomic locus important for acute pathogenesis. J. Virol. **75:**5315–5327.
14. **Marques, S., S. Efstathiou, K. G. Smith, M. Haury, and J. P. Simas.** 2003. Selective gene expression of latent murine gammaherpesvirus 68 in B lymphocytes. J. Virol. **77:**7308–7318.
15. **Moorman, N. J., H. W. Virgin, and S. H. Speck.** 2003. Disruption of the gene encoding the gammaHV68 v-GPCR leads to decreased efficiency of reactivation from latency. Virology **307:**179–190.
16. **Parry, C. M., J. P. Simas, V. P. Smith, C. A. Stewart, A. C. Minson, S. Efstathiou, and A. Alcami.** 2000. A broad spectrum secreted chemokine binding protein encoded by a herpesvirus. J. Exp. Med. **191:**573–578.
17. **Reading, P. C., J. A. Symons, and G. L. Smith.** 2003. A soluble chemokine-binding protein from vaccinia virus reduces virus virulence and the inflammatory response to infection. J. Immunol. **170:**1435–1442.
18. **Roy, D. J., B. C. Ebrahimi, B. M. Dutia, A. A. Nash, and J. P. Stewart.** 2000. Murine gammaherpesvirus M11 gene product inhibits apoptosis and is expressed during virus persistence. Arch. Virol. **145:**2411–2420.
19. **Sambrook, J., E. F. Fritsch, and T. Maniatis.** 1989. Molecular cloning: a laboratory manual, 2nd ed. Cold Spring Harbor Laboratory Press, Cold Spring Harbor, N.Y.
20. **Simas, J. P., D. Swann, R. Bowden, and S. Efstathiou.** 1999. Analysis of murine gammaherpesvirus-68 transcription during lytic and latent infection. J. Gen. Virol. **80**(Pt. 1)**:**75–82.
21. **Stewart, J. P., E. J. Usherwood, A. Ross, H. Dyson, and T. Nash.** 1998. Lung epithelial cells are a major site of murine gammaherpesvirus persistence. J. Exp. Med. **187:**1941–1951.
22. **Sunil-Chandra, N. P., J. Arno, J. Fazakerley, and A. A. Nash.** 1994. Lymphoproliferative disease in mice infected with murine gammaherpesvirus 68. Am. J. Pathol. **145:**818–826.
23. **Sunil-Chandra, N. P., S. Efstathiou, J. Arno, and A. A. Nash.** 1992. Virological and pathological features of mice infected with murine gamma-herpesvirus 68. J. Gen. Virol. **73**(Pt. 9)**:**2347–2356.
24. **Tibbetts, S. A., L. F. van Dyk, S. H. Speck, and H. W. Virgin.** 2002. Immune control of the number and reactivation phenotype of cells latently infected with a gammaherpesvirus. J. Virol. **76:**7125–7132.
25. **Usherwood, E. J., A. J. Ross, D. J. Allen, and A. A. Nash.** 1996. Murine gammaherpesvirus-induced splenomegaly: a critical role for CD4 T cells. J. Gen. Virol. **77**(Pt. 4)**:**627–630.
26. **Usherwood, E. J., D. J. Roy, K. Ward, S. L. Surman, B. M. Dutia, M. A. Blackman, J. P. Stewart, and D. L. Woodland.** 2000. Control of gammaherpesvirus latency by latent antigen-specific $CD8^+$ T cells. J. Exp. Med. **192:**943–952.
27. **Usherwood, E. J., J. P. Stewart, K. Robertson, D. J. Allen, and A. A. Nash.** 1996. Absence of splenic latency in murine gammaherpesvirus 68-infected B-cell-deficient mice. J. Gen. Virol. **77**(Pt. 11)**:**2819–2825.
28. **Usherwood, E. J., K. A. Ward, M. A. Blackman, J. P. Stewart, and D. L. Woodland.** 2001. Latent antigen vaccination in a model gammaherpesvirus infection. J. Virol. **75:**8283–8288.
29. **van Berkel, V., B. Levine, S. B. Kapadia, J. E. Goldman, S. H. Speck, and H. W. Virgin.** 2002. Critical role for a high-affinity chemokine-binding protein in gamma-herpesvirus-induced lethal meningitis. J. Clin. Investig. **109:**905–914.
30. **van Berkel, V., K. Preiter, H. W. Virgin, and S. H. Speck.** 1999. Identification and initial characterization of the murine gammaherpesvirus 68 gene M3, encoding an abundantly secreted protein. J. Virol. **73:**4524–4529.
31. **Virgin, H. W., P. Latreille, P. Wamsley, K. Hallsworth, K. E. Weck, A. J. Dal Canto, and S. H. Speck.** 1997. Complete sequence and genomic analysis of murine gammaherpesvirus 68. J. Virol. **71:**5894–5904.
32. **Virgin, H. W., R. M. Presti, X. Y. Li, C. Liu, and S. H. Speck.** 1999. Three distinct regions of the murine gammaherpesvirus 68 genome are transcriptionally active in latently infected mice. J. Virol. **73:**2321–2332.
33. **Wakeling, M. N., D. J. Roy, A. A. Nash, and J. P. Stewart.** 2001. Characterization of the murine gammaherpesvirus 68 ORF74 product: a novel oncogenic G protein-coupled receptor. J. Gen. Virol. **82:**1187–1197.
34. **Weck, K. E., S. S. Kim, H. W. Virgin, and S. H. Speck.** 1999. B cells regulate murine gammaherpesvirus 68 latency. J. Virol. **73:**4651–4661.
35. **Weck, K. E., S. S. Kim, H. W. Virgin, and S. H. Speck.** 1999. Macrophages are the major reservoir of latent murine gammaherpesvirus 68 in peritoneal cells. J. Virol. **73:**3273–3283.